Structure and Bonding in Linear-bridged Species: Electronic, Raman, and Resonance Raman Spectra of the Trinuclear Dinitrogen-bridged Complex $[\{Cl(PMe_2Ph)_4Re(N_2)\}_2MoCl_4]$

Jeremy R. Campbell, Robin J. H. Clark,* and Martin J. Stead
Christopher Ingold Laboratories, University College London, 20 Gordon Street, London WC1H 0AJ

The electronic and vibrational spectra of the complex $[\{Cl(PMe_2Ph)_4Re(N_2)\}_2MoCl_4]$ have been studied in detail. The Raman spectra have been recorded with a variety of different exciting lines; they were found to be enhanced in the vicinity of the intense absorption bands in the visible region, in particular for the bands at 1 818, 689, and 290 cm^{-1} attributed to the $\nu_1(a_{1g})$,ν(NN), $\nu_2(a_{1g})$,ν(MN), and $\nu_5(a_{1g})$,ν(ReCl) fundamentals, respectively. Raman band excitation profiles for many a_{1g} bands, and approximate force-constant calculations, have been co-ordinated with a proposed molecular orbital scheme for the linear skeleton to provide a coherent picture of the bonding in the complex. The (resonant) electronic bands are assigned to $e_g(\pi) \leftarrow e_u(\pi)$ and $e_u(\pi^*) \leftarrow e_g(\pi)$, $^1A_{2u} \leftarrow {}^1A_{1g}$ transitions of the linear chain, on the bases of Raman band depolarisation ratio measurements.

Dinitrogen is now well known to act as a ligand in the formation of many transition metal complexes. This fact is not only of chemical interest but also of considerable biological interest and helps to shed light on the nitrogen fixation process (the bacterial conversion of atmospheric nitrogen to organic nitrogen compounds). For example, molybdenum is well known to be an essential component of nitrogenase and is thought to be the site of dinitrogen interaction and reduction.[1,2] Chatt and Richards[3] have investigated several dinitrogen complexes of molybdenum in an attempt to discover how dinitrogen may be activated by such ligation. In so doing they make extensive use of the idea of the metal acting as both a σ-acceptor as well as a π-donor and/or π-acceptor.

The simplest types of dinitrogen complexes are the mononuclear ones. A well known example of such a complex is $[Re(PMe_2Ph)_4Cl(N_2)]$, an octahedral complex in which the chloride and dinitrogen ligands are *trans* to each other. Another example is $[Mo(PMe_2Ph)_4(N_2)_2]$ which has the two dinitrogen ligands *cis* to each other. The above rhenium complex is known[3,4] to react with a variety of acceptor molecules to form binuclear dinitrogen complexes of the type $[Re(PMe_2Ph)_4Cl(N_2)A]$ where, for example, $A = CrCl_3(thf)_2$ (thf = tetrahydrofuran), $MoCl_3(thf)_2$, $MoCl_4(OMe)$, or $WCl_4(PMe_2Ph)$. In these complexes the dinitrogen ligand is the bridging ligand, resulting in the formation of Re–N–N–M bridges (M = Cr, Mo, or W).

More recently, it has been shown that the acceptor molecule can sometimes bind to two rhenium units to form a trinuclear, dinitrogen-bridged complex.[3,5] Examples are now known where the acceptor molecules are titanium, molybdenum, or tungsten complexes. One such example is the complex $[\{Cl(PMe_2Ph)_4Re(N_2)\}_2MoCl_4]$, prepared by the reaction of $[Re(PMe_2Ph)_4Cl(N_2)]$ with either $[MoOCl_3]$ or $[Mo(PPh_3)_2Cl_4]$ in dichloromethane.

This complex has been the subject of an *X*-ray crystallographic study[6] which has shown it to have the structure displayed in Figure 1. In this structure there is a linear Cl–Re–N–N–Mo–N–N–Re–Cl backbone with Re–N, N–N, and Mo–N bond lengths of 1.75, 1.28, and 1.99 Å, respectively. The remaining ligands (Cl and PMe_2Ph) complete the octahedral co-ordination of the metal atoms, but more exact details have not been given because of insufficiently accurate data (the errors in the above bond lengths are *ca.* 0.05 Å). Nevertheless, the two Re–N–N–Mo bridges, *trans* to each other, are unambiguously defined. The bond lengths given are also sufficiently accurate to give an indication of the strengths

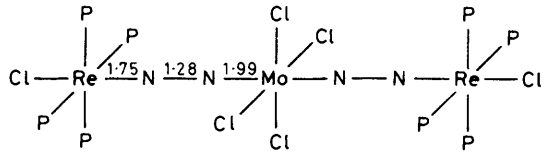

Figure 1. Schematic representation of the structure of $[\{Cl(PMe_2Ph)_4Re(N_2)\}_2MoCl_4]$ (bond distances are in Å)

of the respective bonds. The N–N bond length of 1.28 Å is exactly midway between those found in free nitrogen (1.10 Å)[7] and hydrazine (1.46 Å),[8] thus being strongly indicative of double-bond character. The Re–N bond length of 1.75 Å is also indicative of double-bond character being similar to the M–N bond length in the $[\{RuCl_4(H_2O)\}_2(\mu\text{-}N)]^{3-}$ ion (*ca.* 1.72, Å)[9,10] and the M–O bond lengths of $[M_2OCl_{10}]^{n-}$ (M = Ru Os, W, or Re) ions (*ca.* 1.78—1.87 Å).[11] The Mo–N bond length of 1.99 Å, on the other hand, is considerably closer to that of a single M–N bond {*cf.* the Ru–N bond lengths of *ca.* 2.09—2.17 Å in the $[Ru_3O_2(NH_3)_{14}]^{6+}$ and $[Ru_3O_2(NH_3)_{10}(H_2NCH_2CH_2NH_2)_2]^{6+}$ ions},[12,13] but it is still suggestive of partial double-bond character. Hence, the bonding in these dinitrogen bridges may more accurately be described as Re=N=N–Mo, which is in good agreement with a molecular-orbital scheme (see below) employing the concepts of π bonding.

In view of the fact that the complex $[\{Cl(PMe_2Ph)_4Re(N_2)\}_2MoCl_4]$ (*i*) is structurally similar to the oxygen- and nitrogen-bridged complexes previously studied[11,12,14,15] and (*ii*) is deeply coloured (green), it might be expected that excitation within the contours of electronic bands associated with charge-transfer transitions of the M–N π-bond system would yield resonance Raman (r.R.) spectra. If this were possible, hopefully some insight into the electronic structure of the complex and of related dinitrogen complexes could be gained. Some features of the results have appeared in a preliminary report.[16]

Experimental

The complex $[\{Cl(PMe_2Ph)_4Re(N_2)\}_2MoCl_4]$ was prepared by published methods.[3,4]

The Raman spectra were recorded both on a Spex 1401 spectrometer (1 200 lines mm^{-1}, Bausch and Lomb gratings) and a Spex 14018 R6 spectrometer (1 800 lines mm^{-1}, Jobin-

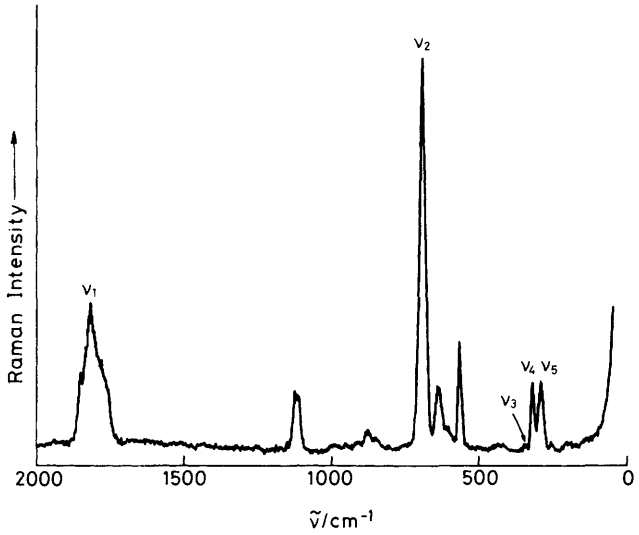

Figure 2. Resonance Raman spectrum of a KBr disc of the complex $[\{Cl(PMe_2Ph)_4Re(N_2)\}_2MoCl_4]$ at *ca.* 80 K: λ_0 = 457.9 nm, power 50 mW, spectral slit width 4 cm^{-1}

Yvon holographic gratings). Samples were either held at room temperature, in which case they were spun at *ca.* 1 200 r.p.m., or at *ca.* 80 K on a copper block attached to a liquid-nitrogen Dewar. Band wavenumbers were determined by reference to the emission lines of neon. Band intensities were assessed from approximate band area measurements (band height × half-width). Intensity data were then corrected for the spectral response of the relevant spectrometer. Both spectrometers were used in conjunction with Coherent Radiation CR 12 and 52 Ar^+ and CR 3000 K or 52 Kr^+ lasers, and with a model 599 dye laser employing the dye LD 700 for the near-i.r. region. Laser powers of ≤40 mW were used throughout.

I.r. spectra were recorded on a Perkin-Elmer 225 spectrometer and the electronic spectra on a Cary 14 spectrometer, the sample being dispersed in KCl or KBr discs, or in dichloromethane solution; the spectrum was the same in all three cases.

Results and Discussion

If the PMe_2Ph ligands are treated as point masses, then the vibrational representation of $[\{Cl(PMe_2Ph)_4Re(N_2)\}_2MoCl_4]$, in D_{4h} nomenclature, is given by the following expression.

$$\Gamma_{vib.} = 7a_{1g} + a_{2g} + 3b_{1g} + 2b_{2g} + 7e_g + a_{1u} + 7a_{2u} + b_{1u} + 3b_{2u} + 9e_u$$

In keeping with the schemes employed previously for other bridged species,[11,12] the Raman-active a_{1g} modes, in decreasing wavenumber order, will be labelled ν_1—ν_7 and the i.r.-active a_{2u} modes likewise, ν_8—ν_{14}.

Resonance Raman and Infrared Spectra.—The r.R. spectrum of $[\{Cl(PMe_2Ph)_4Re(N_2)\}_2MoCl_4]$ recorded with 457.9 excitation at *ca.* 80 K is displayed in Figure 2. Band wavenumbers of both the solid-phase and solution r.R. spectra, depolarisation ratios, and i.r. band wavenumbers are given in Table 1.

The r.R. spectrum of this complex with blue excitation is dominated by two very intense bands which, at *ca.* 80 K, lie at 1 818 and 689 cm^{-1}. The former clearly arises from an N–N stretching fundamental, and is thus assigned to $\nu_1(a_{1g})$, $\nu_{sym.}(NN)$. This assignment is consistent with the double-bond character of the N–N bond (*cf.* free nitrogen, whose fundamental lies at *ca.* 2 330 cm^{-1}). In addition, i.r. bands in the region of 1 800 cm^{-1} have frequently been used to characterise dinitrogen complexes.[3-5] The other band, at 689 cm^{-1}, is assigned to the $\nu_2(a_{1g})$,$\nu_{sym.}$(MN) fundamental, a metal–nitrogen stretching mode involving both Re–N and Mo–N stretching but not (to a first approximation) N–N stretching. This mode is analogous to the $\nu_1(a_{1g})$,$\nu_{sym.}$(RuO) fundamental (827 cm^{-1}) of ruthenium red;[12] in both cases the principal movement is of the bridging ligand between the metal atoms. The band at 1 818 cm^{-1} also exhibits two shoulders at 1 762 and 1 853 cm^{-1}, possibly due to solid-state effects (since they are not observed in solution spectra).

Two further bands of medium intensity at 318 and 290 cm^{-1} are assigned to $\nu_4(a_{1g})$,$\nu_{sym.}$(MoCl), and $\nu_5(a_{1g})$,$\nu_{sym.}$(ReCl), respectively; the relative wavenumbers of these modes are based upon the established dependence of metal–ligand stretching frequencies on metal-ion oxidation state, *i.e.* $\nu(M^{IV}Cl) > \nu(M^{I}Cl)$,[17] and upon excitation profile studies (see below).

If the PMe_2Ph ligands are treated as point masses, then three more totally symmetric modes would be expected, each giving rise to a Raman band. Two of them, ν_3 and ν_6, involve Re–P stretching and N–Re–P bending, respectively, while the third, ν_7, involves M–N stretching. On the bases of many i.r. studies of gold–phosphine complexes,[18] ν(AuP) has been considered to give rise to bands at *ca.* 359—381 cm^{-1}. Accordingly, the weak band at 347 cm^{-1} is assigned to $\nu_3(a_{1g})$,$\nu_{sym.}$(ReP). The bending mode $\nu_6(a_{1g})$,$\delta_{sym.}$(NReP) would thus be expected to lie at about half this wavenumber, but no

Table 1. Wavenumbers (cm^{-1}) of the bands observed in the r.R. and i.r. spectra of the complex $[\{Cl(PMe_2Ph)_4Re(N_2)\}_2MoCl_4]$

	r.R.			
		Solid		
Assignment	Solution [a]	r.t. [b]	l.t. [c]	I.r.
$\nu_1(a_{1g})$,$\nu_{sym.}$(NN)	1 800 (0.24)	1 809	1 762 (sh), 1 817.6vs,br, 1 853 (sh)	
$\nu_8(a_{2u})$,$\nu_{asym.}$(NN)				1 795s,br, 1 830 (sh)
				1 432m
	1 111 (0.22)	1 114	1 117.3m	1 110m,br
PMe_2Ph modes	876 (0.21)	865	876w	905s, 940m
				700m, 743m
$\nu_2(a_{1g})$,$\nu_{sym.}$(MN)	682 (0.25)	676	689.2vs	
$\nu_9(a_{2u})$,$\nu_{asym.}$(MN)?				675w
	630 (0.35)	635	635.4m	630m
	560 (0.27)	555	563.8m	542w
PMe_2Ph modes				496w
	419 (0.22)	425	*ca.* 420w	415m
$\nu_3(a_{1g})$,$\nu_{sym.}$(ReP)			347w	
$\nu_4(a_{1g})$,$\nu_{sym.}$(MoCl)	311 (0.26)	315	317.9m	
$\nu_1(a_{2u})$,$\nu_{asym.}$(MoCl)?				310w
$\nu_5(a_{1g})$,$\nu_{sym.}$(ReCl)	*d*	285	289.8m	
PMe_2Ph modes			200w, 253w	

[a] Dichloromethane solution; depolarisation ratios are given in parentheses for λ_0 = 457.9 nm. [b] r.t. = Room temperature. [c] l.t. = Low temperature. [d] Obscured by solvent.

firm assignment can be made since the wavenumbers of the two weak bands observed at 253 and 200 cm^{-1} are higher than expected if they were to be so attributed. This leaves the assignment of $\nu_7(a_{1g})$, $\nu_{sym.}(MN)$. The corresponding mode of ruthenium red, $\nu_{sym.}(RuO)$, lies at 150 cm^{-1} [12] but a lower wavenumber than this might be expected here since PMe_2Ph is heavier than NH_3, and since the Mo–N bonds in the title complex have a lower bond order than the Ru–O bonds in ruthenium red. However, no band was observed around 100 cm^{-1}.

The bands referred to above are all polarised (as shown by solution r.R. spectra) in agreement with their being assigned to totally symmetric modes of the $Re_2MoP_8Cl_6N_4$ skeleton. Thus, in order to assign the remaining bands (which are also polarised) in the r.R. spectra, the methyl and phenyl substituents of the PMe_2Ph ligands must be taken into account. The bands in question lie at 1 117, 876, 635, 564, and 420 cm^{-1} and, except for the weak ones at 876 and 420 cm^{-1}, are of medium intensity. The band at 876 cm^{-1} is likely to arise from a C–H wagging mode, but the others from modes which involve C–P stretching. The bands at 1 117, 876, 635, and 420 cm^{-1} all have obvious counterparts in the vibrational spectra of free PMe_2Ph [19] but the band at 564 cm^{-1} is more difficult to assign. No Raman bands have been reported in the range 500—600 cm^{-1} for free PMe_2Ph, nor for PR_3 complexes (R = Me,[20,21] Et,[22] or Ph [23]), although such bands do appear in the i.r. spectra of PPh_3 complexes.[23] Additional bands would be expected to arise from rocking modes, but these would lie at *ca.* 200 cm^{-1}. Such modes were observed for PMe_3 complexes,[20,21] assigned to $\rho(PC_3)$ and $\delta(PC_3)$, which probably account for the bands observed at 253 and 200 cm^{-1} mentioned above.

The i.r. spectrum of $[\{Cl(PMe_2Ph)_4Re(N_2)\}_2MoCl_4]$ is dominated by bands due to the PMe_2Ph ligands but one important exception is the band at 1 795 cm^{-1}, assigned to $\nu_8(a_{2u}),\nu_{asym.}(NN)$. This agrees reasonably well with the value of 1 800 cm^{-1} reported by Chatt and Richards [3] for a Nujol mull (the only i.r. band wavenumber given by these authors). A shoulder at *ca.* 1 830 cm^{-1} was also observed on the band at 1 795 cm^{-1} possibly due to either an impurity or solid-state effects. Of the lower wavenumber bands, most are due to the PMe_2Ph ligands but some arise from M–N stretching and M–N–N bending modes; $\nu_9(a_{2u}),\nu_{asym.}(MN)$ is likely to give rise to a band in the range 600—700 cm^{-1} (*cf.* ν_2) while the e_u modes $\delta(ReNN)$ and $\delta(MoNN)$ are likely to lie at *ca.* 300—500 cm^{-1} {*cf.* $\delta(MOM)$ of $[M_2OX_{10}]^{n-}$ ions}.[11,15]

Force-constant Calculations.—A very simplified force-constant treatment was carried out on the complex $[\{Cl(PMe_2Ph)_4Re(N_2)\}_2MoCl_4]$ in order to aid the assignments of its r.R. and i.r. bands and the interpretation of excitation profiles (see below).

The same simplifications were made as for ruthenium red,[12] namely the assumption of D_{4h} symmetry and the consideration of axial a_{1g} and a_{2u} modes only. The construction of the a_{1g} and a_{2u} *G*-matrix blocks is described elsewhere.[24] Included in the treatment of the a_{1g} block were the axial symmetry co-ordinates, S_1—S_5, involving Mo–N, N–N, Re–N, and Re–Cl stretches and the N–Re–P deformation, respectively. The equatorial modes were omitted (the Mo–Cl and Re–P stretches, related to F_{66} and F_{77}) and the PMe_2Ph ligands were treated as points of mass 31. A similar set of co-ordinates was employed for the a_{2u} block (S_8—S_{12} respectively).

A modified general quadratic valence force field was employed, similar to that used for ruthenium red.[12] Of the ten off-diagonal *F*-matrix elements of each block, five were set equal to zero. These consisted of three stretch–stretch interactions, in which no common atom was involved, and two stretch–bend interactions, in which no common bond was involved. Hence, in terms of valence force constants, the *F*-matrix elements are given by F_{11}—F_{45}.

Table 2. Force constants and calculated band wavenumbers for the a_{1g} and a_{2u} axial fundamentals for the complex $[\{Cl(PMe_2Ph)_4Re(N_2)\}_2MoCl_4]$

F_{11} */mdyn Å^{-1}	3.9	$F_{12}(F_{89})$/mdyn Å^{-1}	1.5
$F_{22}(F_{99})$/mdyn Å^{-1}	14.9	$F_{23}(F_{9\,10})$/mdyn Å^{-1}	1.5
$F_{33}(F_{10\,10})$/mdyn Å^{-1}	4.8	$F_{34}(F_{10\,11})$/mdyn Å^{-1}	0.9
$F_{44}(F_{11\,11})$/mdyn Å^{-1}	2.3	$F_{35}(F_{10\,12})$/mdyn rad^{-1}	−0.8
$F_{55}(F_{12\,12})$/ mdyn Å rad^{-2}	1.4	$F_{45}(F_{11\,12})$/mdyn rad^{-1}	0.4
F_{88} */mdyn Å^{-1}	2.1		
$\tilde{\nu}_1(a_{1g})$/cm^{-1}	1 848	$\tilde{\nu}_8(a_{2u})$/cm^{-1}	1 821
$\tilde{\nu}_2(a_{1g})$/cm^{-1}	736	$\tilde{\nu}_9(a_{2u})$/cm^{-1}	671
$\tilde{\nu}_5(a_{1g})$/cm^{-1}	338	$\tilde{\nu}_{12}(a_{2u})$/cm^{-1}	338
$\tilde{\nu}_6(a_{1g})$/cm^{-1}	216	$\tilde{\nu}_{13}(a_{2u})$/cm^{-1}	243
$\tilde{\nu}_7(a_{1g})$/cm^{-1}	100	$\tilde{\nu}_{14}(a_{2u})$/cm^{-1}	211

* $f(MoN) = \frac{1}{2}(F_{11} + F_{88}) = 3.0$ mdyn Å^{-1}; $f(MoN/MoN) = \frac{1}{2}(F_{11} - F_{88}) = 0.9$ mdyn Å^{-1}. 1 dyn = 10^{-5} N.

$$
\begin{aligned}
F_{11} &= f(MoN) + f(MoN/MoN)\\
F_{22} = F_{99} &= f(NN)\\
F_{33} = F_{10\,10} &= f(ReN)\\
F_{44} = F_{11\,11} &= f(ReCl)\\
F_{55} = F_{12\,12} &= \tfrac{1}{2}r(ReP)^2[f(NReP) + f(ClReP)]\\
F_{88} &= f(MoN) - f(MoN/MoN)\\
F_{12} = F_{89} &= f(MoN/NN)\\
F_{23} = F_{9\,10} &= f(ReN/NN)\\
F_{34} = F_{10\,11} &= f(ReN/ReCl)\\
F_{35} = F_{10\,12} &= -\sqrt{2}r(ReP)f(ReN/NReP)\\
F_{45} = F_{11\,12} &= \sqrt{2}r(ReP)f(ReCl/ClReP)
\end{aligned}
$$

The value for $f(NN)$ was taken to be two-thirds of that derived from the vibrational wavenumber of free N_2 (*ca.* 2 330 cm^{-1}). The values for the remaining force constants were based upon the results of the calculations carried out on the $[Re_2OCl_{10}]^{n-}$ ions.[11,15] The force constants $f(ReX)$ and $f(XReP)$ (X = N or Cl) were taken from the mean values of $f(ReY)$ and $f(YReCl_{eq})$, respectively (Y = O or Cl). Similarly, the corresponding interaction force constants were also transferred from the binuclear ions. The $f(MoN)$ force constant was assigned a value intermediate between those of double and single bonds on account of the $r(MoN)$ bond length indicating a similarly intermediate bond order. The $f(MoN/MoN)$ interaction force constant was set equal to $0.3\,f(MoN)$, since a similar ratio was found for $f(MO/MO):f(MO)$ of $[M_2OCl_{10}]^{n-}$ ions and ruthenium red. Finally, the $f(MoN/NN)$ and $f(ReN/NN)$ force constants were taken to be about a tenth of the $f(NN)$ value.

The actual values used for the *F*-matrix elements are given in Table 2, which also includes the wavenumbers of the a_{1g} and a_{2u} bands as predicted by the above field. In view of the substantial assumptions made in these calculations, which were not refined, the agreement between observed (Table 1) and calculated (Table 2) band wavenumbers is adequate for the present purposes (a more detailed discussion of this analysis and in particular, its relation to that of ruthenium red, is given elsewhere [24]). From the analysis, the potential energy distribution of the a_{1g} normal modes comes out to be of the form shown below (entries in italic signify that the corresponding entries in the *L*-matrix are negative). From this it can be seen that Q_1 is relatively pure S_2, that Q_5 is relatively pure S_4, but that Q_2, Q_6, and Q_7 are extensive mixtures of

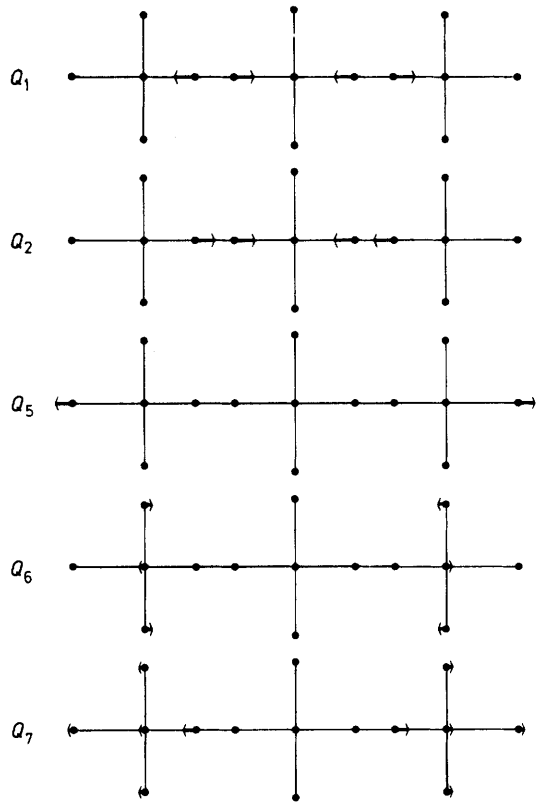

Figure 3. Representation of the axial a_{1g} normal co-ordinates, based on the results of the approximate force-constant calculations

	S_1	S_2	S_3	S_4	S_5
Q_1	5	87	7	0	0
Q_2	44	0	55	0	0
Q_5	0	0	6	94	0
Q_6	1	0	17	7	74
Q_7	58	2	37	0	4

symmetry co-ordinates. Indeed, the mixing of S_1, S_3, S_4, and S_5 into Q_2, Q_5, Q_6, and Q_7 is very similar to that found for the corresponding modes of ruthenium red.[12] The forms of the normal co-ordinates calculated on the basis of the above analysis are shown in Figure 3. As can be seen, Q_1 and Q_2 may be described as N–N and M–N stretching modes, respectively, and Q_5 and Q_6 as Re–Cl stretching and N–Re–P bending modes, respectively. The mode Q_7 appears to involve N–N stretching in which the ReP_4ClN groups move as a whole, thus accounting for the low wavenumber expected for this mode.

Excitation Profiles, Electronic Spectra, and Molecular Orbital Scheme.—The excitation profiles of several Raman bands of the complex $[\{Cl(PMe_2Ph)_4Re(N_2)\}_2MoCl_4]$ at *ca.* 80 K have been determined by reference to the intensity of the $\nu_1(a_1)$ band of potassium sulphate and are displayed, along with the electronic absorption spectrum, in Figure 4. Excitation at wavelengths shorter than 457.9 nm resulted in thermal and/or photochemical decomposition of the sample. Some of the band profiles could be monitored to the red-i.r. limit of 799.3 nm; the remainder could not, either because they were too weak or, as in the case of ν_1, because the photomultiplier was insufficiently sensitive, at an 1 818 cm^{-1} shift from lines of longer wavelengths than 647.1 nm, to permit reliable intensity studies to be carried out.

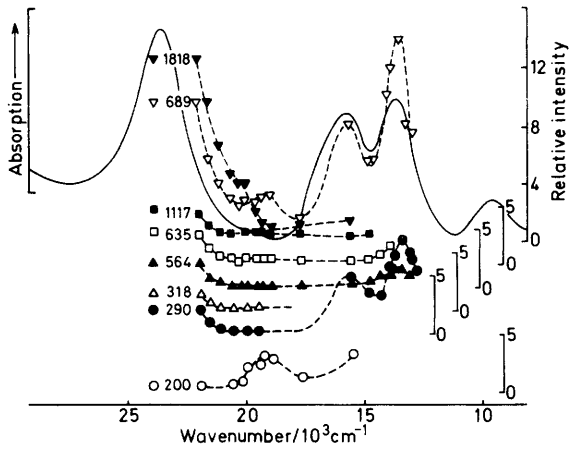

Figure 4. Excitation profiles of the a_{1g} fundamentals of the title complex, measured relative to the $\nu_1(a_1)$ band of K_2SO_4 as standard at *ca.* 80 K, together with the absorption spectrum of the complex

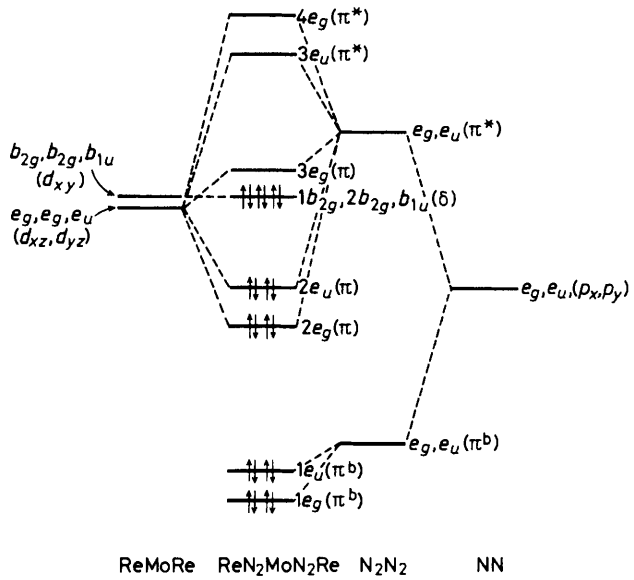

Figure 5. Proposed molecular orbital scheme for the complex

As can be seen from Figure 4, the profiles which display the greatest enhancement at resonance with the doublet of strong absorption bands at 13 500—15 600 cm^{-1} are those attributed to $\nu_2,\nu_{sym.}(MN)$ and $\nu_{5,sym.}(ReCl)$, and with the strong absorption band at 23 300 cm^{-1} are those attributed to $\nu_1,\nu_{sym.}(NN)$, ν_2, and ν_5. These effects strongly suggest that the electronic bands are associated with transitions involving the axial π-bond system.

A molecular orbital scheme for the complex is given in Figure 5. An eclipsed D_{4h} structure has been adopted and only the *d* orbitals of the metal atoms and *p* orbitals of the nitrogen atoms have been considered. The scheme is similar to that employed for ruthenium red. In the case of the complex $[\{Cl(PMe_2Ph)_4Re(N_2)\}_2MoCl_4]$, however, the nitrogen *p* orbitals interact with each other to form either bonding or antibonding molecular orbitals. The separation in energy between these orbitals is large and only the antibonding ones are expected to match approximately, and thus to interact with, the metal *d* orbitals to any great extent. The two e_g and one e_u combinations of metal d_{xz} and d_{yz} orbitals interact with

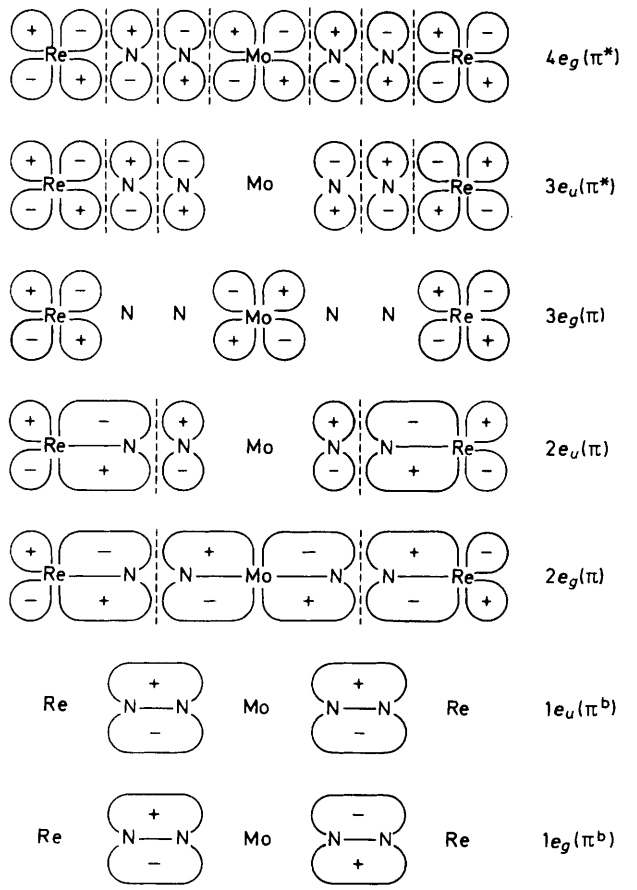

Figure 6. The axial e_g and e_u π-molecular orbitals of the complex (schematic). No attempt has been made to allow for the different relative sizes of the various orbitals shown

the $e_g(\pi^*)$ and $e_u(\pi^*)$ molecular orbitals of dinitrogen to form a set of $1e_g(\pi^b)$, $1e_u(\pi^b)$, $2e_g(\pi)$, $2e_u(\pi)$, $3e_g(\pi)$, $3e_u(\pi^*)$, and $4e_g(\pi^*)$ molecular orbitals of the complex. The $1e_u(\pi^b)$ and $1e_u(\pi^b)$ molecular orbitals of dinitrogen, however, remain essentially localised on the dinitrogen ligands (see Figure 6). The Re–Mo separation (5.02 Å) is very large and so the two b_{2g} and one b_{1u} combinations of d_{xy} orbitals on the metal atoms are effectively non-bonding δ molecular orbitals. Ideas similar to these have been used previously to describe the bonding in the binuclear dinitrogen complexes $[Ru_2(NH_3)_{10}(N_2)][BF_4]_4$ [25] and $[Re(PMe_2Ph)_4Cl(N_2)A]$ [3,4] [A = $CrCl_3(thf)_2$, $MoCl_3(thf)_2$, $MoCl_4(OMe)$, or $WCl_4(PMe_2Ph)$].

The distribution of the 22 valence electrons of the complex $[\{Cl(PMe_2Ph)_4Re(N_2)\}_2MoCl_4]$ is indicated in Figure 5 for the ground state, which is formally designated to be $Re^I(d^6)$-$N_2(p^4)Mo^{IV}(d^2)N_2(p^4)Re^I(d^6)$. From this, bond order may be estimated for the Re–N, N–N, and Mo–N bonds, remembering that the normal σ-bond framework already accounts for a bond order of unity. Thus the N–N bonds are made triple by the filling of the $1e_g(\pi^b)$ and $1e_u(\pi^b)$ orbitals but a decrease in NN bond order results from the filling of the $2e_g(\pi)$ and $2e_u(\pi)$ orbitals, which are antibonding with respect to the N–N bonds. These $2e_g(\pi)$ and $2e_u(\pi)$ orbitals, which contain four electrons each, are localised over six and four bonds, respectively, and so result in N–N bond-order decreases of $\frac{1}{3}$ and $\frac{1}{2}$, respectively. Thus the net N–N bond order is $3 - \frac{1}{3} - \frac{1}{2} = 2\frac{1}{6}$. It can also easily be seen that the bond orders of the Re–N and Mo–N bonds are predicted by this method to be $1 + \frac{1}{3} + \frac{1}{2} = 1\frac{5}{6}$ and $1 + \frac{1}{3} = 1\frac{1}{3}$, respectively. Thus the bonding in the complex can approximately be described as Re=N=N–Mo, or perhaps Re=N=N···Mo, which agrees very well with that predicted by bond length data [r(Re–N) = 1.75, r(N–N) = 1.28, r(Mo–N) = 1.99 Å], and supports the assumptions made in the force-constant calculations (Table 2).

On the basis of this scheme, the ground-state electronic configuration is likely to be $(1e_g^b)^4(1e_u^b)^4(2e_g)^4(2e_u)^4(1b_{2g})^2$-$(b_{1u})^2(2b_{2g})^2(3e_g)^0$, which gives rise to a $^1A_{1g}$ ground term. Other possibilities would arise if the $3e_g(\pi)$ orbital were not placed significantly higher in energy than the three δ orbitals, but if this were the case there would be up to four unpaired electrons, a situation which would not be consistent with the known diamagnetism [3] of the complex. The lowest two allowed transitions of z-polarisation are thus $3e_g \leftarrow 2e_u$ and $3e_u \leftarrow 2e_g$, which are each allowed *via* their $^1A_{2u} \leftarrow {}^1A_{1g}$ components. Other possibilities are that the electron is transferred from a δ orbital, *i.e.* $3e_g \leftarrow b_{1u}$, $^1E_u \leftarrow {}^1A_{1g}$ or $3e_u \leftarrow b_{2g}$, $^1E_u \leftarrow {}^1A_{1g}$ (two such transitions). All of these transitions are allowed, but only *via* an E_u component and would thus be x,y-polarised.

If the resonant electronic transitions are z-polarised then the depolarisation ratios of these bands should be $\frac{1}{3}$ on resonance.[26] It was found that those bands (1 818, 1 117, 689, 635, 564, and 311 cm^{-1}) for which depolarisation ratios could be measured gave ρ values for both 457.9 and 647.1 nm excitation of between 0.24 and 0.42, indication that (consistent with the axial nature of the Raman bands which display the most marked resonance enhancement) the resonant electronic bands are indeed z-polarised. We thus suggest that the doublet of absorption bands at 13 500—15 600 cm^{-1} is the $3e_g \leftarrow 2e_u$, $^1A_{2u} \leftarrow {}^1A_{1g}$ transition, and that the absorption band at 23 300 cm^{-1} is the $3e_u \leftarrow 2e_g$, $^1A_{2u} \leftarrow {}^1A_{1g}$ transition. The weak absorption band at 9 500 cm^{-1} may thus tentatively be assigned to the x,y-polarised $3e_g \leftarrow \delta$ transitions.

Although the reason for the doublet nature of the $3e_g \leftarrow 2e_u$ transition is uncertain, it is possible that the band at 15 600 cm^{-1} is a vibronic side-band to the band at 13 500 cm^{-1} since the wavenumber separation (2 100 cm^{-1}) would correspond to one quantum of ν_1 (the NN stretch) in the excited state. Consistent with this idea, the values both of ν_1 (1 818 cm^{-1}) and of the NN bond order ($2\frac{1}{6}$) in the ground state are less than the corresponding values in the excited state (2 100 cm^{-1} and $2\frac{2}{3}$, respectively) and less still than the values for free nitrogen (2 330 cm^{-1} and 3, respectively). On this basis, the band at 15 600 cm^{-1} results from vibronic coupling of the two lowest-lying $^1A_{2u}$ states *via* totally symmetric normal coordinates, principally ν(NN). Such a situation normally gives rise to a r.R. excitation profile in which there are two maxima of equal intensity corresponding to 0_g–0_e and 0_g–1_e resonances. The lower Raman intensity observed in the 0_g–1_e region could be due either to non-adiabatic vibronic coupling [27] or to interference between the A-term (Franck–Condon) and B-term (Herzberg–Teller) contributions to the transition polarizability.[28] Since the $^1A_{2u}$ states are well separated (by *ca.* 10 000 cm^{-1}) non-adiabatic effects will be small and it is therefore more likely that the 0_g–0_e/0_g–1_e asymmetry in the excitation profiles may be ascribed to A-term/B-term interference. Vibronic side-bands of this sort are known for the Q-band of haemoglobin [29] and for a variety of tris-bidentate complexes of iron(III).[30] The difficulty with this explanation, however, is that one would expect the vibronic sidebands of the other monitored modes to appear at wavenumber separations less than 2 100 cm^{-1}, and this is not the case.

By reference to Figure 6 it is evident that transfer of an electron from the $2e_u(\pi)$ to the $3e_g(\pi)$ orbital would result primarily in a lengthening of the Re–N bond and a shortening of the N–N bond, while transfer of an electron from the $2e_g(\pi)$ to the $3e_u(\pi^*)$ orbital would result primarily in a length-

ening of both the Re–N and Mo–N bonds. Moreover, as a consequence of either of these transitions, both the effective positive charge on the rhenium atoms and their π-acceptor capability will be affected, and hence the strength of the Re–Cl bonds (also axial) will be affected. Since, according to r.R. theory,[31] the mode(s) most enhanced at resonance with an electric-dipole allowed transition is (are) the totally symmetric one(s) most involved in changing the molecule from the ground-state geometry to the excited-state one, it follows that modes such as ν_1, ν_2, and ν_5 should indeed be the ones most enhanced at resonance with the $\pi \leftarrow\!\!- \pi$ transitions mentioned above. Moreover, the lack of overtones at resonance is fully consistent with the *A*-term small-displacement model for r.R. scattering, as enunciated in detail in the case of ruthenium red and ruthenium brown.[32]

Conclusions

The r.R. results thus allow not only the formulation of a reasonable and consistent picture of the bonding in this complex, but also the assignment of the intense bands in the electronic spectrum to metal-to-nitrogen π-type transitions of the linear backbone.

Acknowledgements

We thank Dr. J. R. Dilworth for the synthesis of the complex. Two of us (J. R. C. and M. J. S.) thank the Science and Engineering Research Council for financial support.

References

1 R. R. Eady, C. Kennedy, B. E. Smith, R. N. F. Thorneley, M. G. Yates, and J. R. Postgate, *Biochem. Soc. Trans.*, 1975, **3**, 488.
2 W. Zumft and L. E. Mortenson, *Biochim. Biophys. Acta*, 1975, **416**, 1.
3 J. Chatt and R. L. Richards, *J. Less-Common Met.*, 1977, **54**, 477.
4 J. Chatt, R. C. Fay, and R. L. Richards, *J. Chem. Soc. A*, 1971, 702.
5 R. Robson, *Inorg. Chem.*, 1974, **13**, 475.
6 P. D. Chadwick, J. Chatt, R. H. Crabtree, and R. L. Richards, *J. Chem. Soc., Chem. Commun.*, 1975, 351.
7 P. G. Wilkinson and N. B. Houk, *J. Chem. Phys.*, 1956, **24**, 528.
8 'Interatomic Distances,' Spec. Publ. No. 11, The Chemical Society, London, 1958.
9 M. Ciechanowicz and A. C. Skapski, *J. Chem. Soc. A*, 1971, 1792.
10 R. J. D. Gee and H. M. Powell, *J. Chem. Soc. A*, 1971, 1795.
11 J. R. Campbell and R. J. H. Clark, *Mol. Phys.*, 1978, **36**, 1133.
12 J. R. Campbell, R. J. H. Clark, W. P. Griffith, and J. P. Hall, *J. Chem. Soc., Dalton Trans.*, 1980, 2228.
13 P. M. Smith, T. Fealey, J. E. Earley, and J. V. Silverton, *Inorg. Chem.*, 1971, **10**, 1943.
14 R. J. H. Clark, M. L. Franks, and P. C. Turtle, *J. Am. Chem. Soc.*, 1977, **99**, 2473.
15 J. R. Campbell and R. J. H. Clark, *J. Chem. Soc., Faraday Trans. 2*, 1980, 1103.
16 J. R. Campbell, R. J. H. Clark, and J. R. Dilworth, *J. Chem. Soc., Chem. Commun.*, 1980, 772.
17 R. J. H. Clark, *Spectrochim. Acta*, 1965, **21**, 955.
18 C. A. McAuliffe, R. V. Parish, and P. D. Randall, *J. Chem. Soc., Dalton Trans.*, 1979, 1730.
19 J. Goubeau and D. Langhardt, *Z. Anorg. Allg. Chem.*, 1963, **338**, 163.
20 P. L. Goggin and J. R. Knight, *J. Chem. Soc., Dalton Trans.*, 1973, 1489.
21 P. L. Goggin, R. J. Goodfellow, S. R. Haddock, J. R. Knight, F. J. S. Reed, and B. F. Taylor, *J. Chem. Soc., Dalton Trans.*, 1974, 523.
22 J. H. S. Green, *Spectrochim. Acta, Part A*, 1968, **24**, 137.
23 G. B. Deacon and J. H. S. Green, *Spectrochim. Acta, Part A*, 1968, **24**, 845.
24 J. R. Campbell, Ph.D. Thesis, University College, London, 1980.
25 I. M. Treitel, M. T. Flood, R. E. Marsh, and H. B. Gray, *J. Am. Chem. Soc.*, 1969, **91**, 6512.
26 O. S. Mortensen and S. Hassing, in 'Advances in Infrared and Raman Spectroscopy,' eds. R. J. H. Clark and R. E. Hester, Heyden, London, 1980, vol. 6, p. 1.
27 G. J. Small and E. S. Yeung, *Chem. Phys.*, 1975, **9**, 379.
28 R. J. H. Clark and T. J. Dines, *Chem. Phys. Lett.*, 1981, **79**, 321.
29 T. G. Spiro and T. M. Loehr, in 'Advances in Infrared and Raman Spectroscopy,' eds. R. J. H. Clark and R. E. Hester, Heyden, London, 1975, vol. 1, p. 98.
30 R. J. H. Clark, P. C. Turtle, D. P. Strommen, B. Streusand, J. Kincaid, and K. Nakamoto, *Inorg. Chem.*, 1977, **16**, 84.
31 Y. Nishimura, A. Y. Hirakawa, and M. Tsuboi, in 'Advances in Infrared and Raman Spectroscopy,' eds. R. J. H. Clark and R. E. Hester, Heyden, London, 1978, vol. 5, p. 217.
32 R. J. H. Clark and T. J. Dines, *Mol. Phys.*, 1981, **42**, 193.

Received 10*th January* 1983; *Paper* 3/035